National Research
Tomsk
State University

Faculty of Physics
Laboratory of theoretical &
mathematical physics

HELICAL METAMATERIALS WITH STRONG SPATIAL DISPERSION

P.O. Kazinski, P.S. Korolev

Based on

J. Phys. A: Math.Theor., *58*(9), 095701 (2025)

Phys. Rev. B 114(10), 105405 (2026).

INTRODUCTION. CHIRAL MATERIALS

Def. Helical media are media with a permittivity tensor that is invariant under simultaneous rotation and translation along the axis of rotation.

$$\hat{R}_\psi \hat{T}_{\psi/q} \hat{\varepsilon} (\hat{R}_\psi \hat{T}_{\psi/q})^{-1} = \hat{\varepsilon}, \quad \forall \psi \in \mathbb{R}\,. \qquad (1)$$

Helical media include:

- Cholesteric liquid crystals
- C*- smectics
- Q-plates
- Helical defects in ordered media
- Helical metamaterials

Applications: notch filters, polarization converters, orbital angular momentum converters, etc.

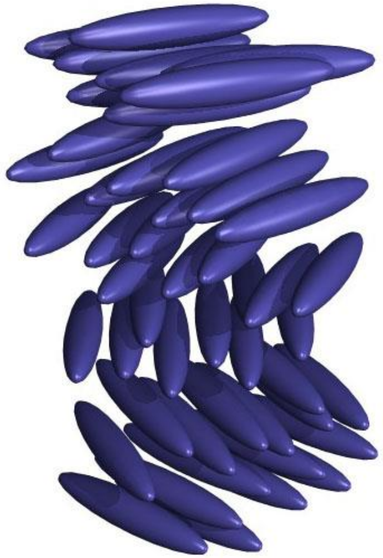


Fig. 1
Cholesteric liquid crystals structure

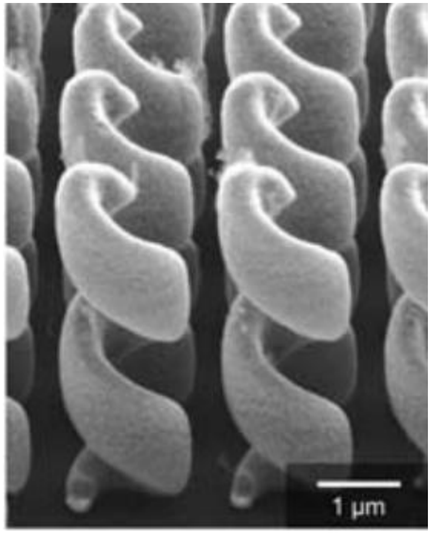


Fig. 2
Helical metamaterial

PROBLEM STATEMENT.
HELICAL METAMATERIALS WITH SPATIAL DISPERSION

A metamaterial composed of an array of ordered metallic spirals is considered.

Its electromagnetic properties are described by Maxwell's equations

$$(\mathrm{rot}^2_{ij} - k_0^2\hat{\varepsilon}_{ij})A_j = 0, \qquad \hat{k}_i(\hat{\varepsilon}_{ij}A_j) = 0, \qquad \hat{k}_i := -i\partial/\partial x_i, \tag{2}$$

where A_j is electromagnetic potential. And k_0 is energy.

The electromagnetic field excites currents in the spiral wires, which in turn affects the electromagnetic properties of the material - this is a manifestation of strong spatial dispersion (or non-locality) in the system.

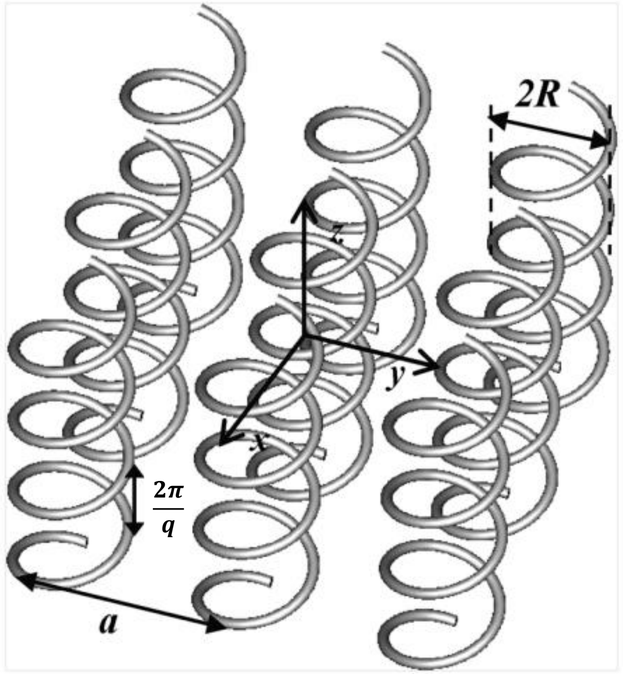


Fig. 3 An array of ordered metallic spirals.

How is the permittivity tensor structured in this case $\hat{\varepsilon}_{ij}$?

Classical approach: homogenization procedure. In this case, information about the helical nature of the material is **lost**.

EFFECTIVE FIELD THEORY APPROACH

Tangent vector to the helix

$$\boldsymbol{\tau}(z) = \cos\alpha \mathbf{e}_3 + \sin\alpha \mathbf{d}(z), \qquad \mathbf{d}(z) = (\cos(qz), \sin(qz), 0)^T, \quad \alpha \in [0, \pi/2]. \tag{3}$$

Where α is the spiral angle, and q determines the helix pitch.

The effective permittivity tensor must be constructed in terms of vectors $\boldsymbol{\tau}, \boldsymbol{k}$ *and invariant tensors* $\delta_{ij}, \epsilon_{ijk}$.

By requiring the symmetry properties to be satisfied and using the available set of invariant tensors, we can expand the denominators of the Weyl symbol of the operator $\hat{\varepsilon}_{ij}$ near the plasmon resonance in the leading order of $\boldsymbol{k}$ as follow

$$\varepsilon_{ij}(k_0; \mathbf{x}, \mathbf{k}) = \varepsilon \left[\delta_{ij} - \frac{\omega_p^2 \tau_i \tau_j}{\varepsilon_h k_0^2 - m^2 - v^2(\boldsymbol{\tau}\mathbf{k})^2 - b^2\mathbf{k}^2} \right]. \tag{4}$$

The kernel of the permittivity operator $\hat{\varepsilon}_{ij}$ reads as

$$K_{ij}(k_0; \mathbf{x}, \mathbf{x}') = \varepsilon_h \left[\delta_{ij} - \tau_i(z) \frac{\omega_p^2}{\omega_0^2 - v^2(\boldsymbol{\tau}(z)\hat{\mathbf{k}})^2} \tau_j(z') \right] \delta(\mathbf{x} - \mathbf{x}'). \tag{5}$$

EFFECTIVE FIELD THEORY APPROACH

The presence of strong spatial dispersion, manifesting itself as a pole in the permittivity tensor, indicates the presence of an additional degree of freedom – a plasmon field propagating along the conducting spirals.

By introducing this field Ψ into the theory, one can rewrite Maxwell's equations in a singularity-free form

$$\begin{aligned}(\omega_0^2 - v^2(\boldsymbol{\tau}\hat{\mathbf{k}})^2)\Psi + \omega_0\omega_p(\boldsymbol{\tau}\mathbf{A}) = 0,\\ (\omega_0^2 - \mathrm{rot}^2)\mathbf{A} + \omega_0\omega_p\Psi\boldsymbol{\tau} = 0\,.\end{aligned} \tag{6}$$

Boundary conditions for a sample of thickness L

$$[\mathbf{A}_\perp]_{z=0} = [\mathbf{A}_\perp]_{z=L} = 0, \qquad [\mathrm{rot}\,\mathbf{A}_\perp]_{z=0} = [\mathrm{rot}\,\mathbf{A}_\perp]_{z=L} = 0 \qquad \Psi(0) = \Psi(L) = 0\,. \tag{7}$$

Using translational invariance in the plane xy

$$\mathbf{A}(\mathbf{x}) = e^{i\mathbf{k}_\perp\mathbf{x}_\perp}\mathbf{A}(z), \qquad \Psi(\mathbf{x}) = e^{i\mathbf{k}_\perp\mathbf{x}_\perp}\Psi(z). \tag{8}$$

Note. It is possible to reduce the system to the form of a multichannel Schrödinger equation in the presence of closed channels

$$\left[\hat{k}_3 M_0 \hat{k}_3 + \frac{1}{2}(\hat{k}_3 M_1 + M_1\hat{k}_3) + M_2\right]W = 0\,. \tag{9}$$

Theorem. The S matrix in the subspace of open channels is unitary.

[P. O. Kazinski and P. S. Korolev, Proc. R. Soc. A **480**, (2024).]

PARAXIAL APPROXIMATION

The system allows for analytical consideration in the case of normal propagation of electromagnetic waves, i.e. $k_\perp = 0$.

Maxwell's equations are reduced to a system of ODEs

$$\begin{aligned}
\omega_0^2 a_+ - \hat{k}_3^2 a_+ + \frac{\omega_p \omega_0}{\sqrt{2}} \sin\alpha e^{i\theta} \tilde{\Psi} = 0, \\
\omega_0^2 a_- - \hat{k}_3^2 a_- + \frac{\omega_p \omega_0}{\sqrt{2}} \sin\alpha e^{-i\theta} \tilde{\Psi} = 0, \\
\left[\omega_0^2 - (\omega_p^2 + v^2 \hat{k}_3^2)\cos^2\alpha\right] \tilde{\Psi} + \frac{\omega_p \omega_0}{\sqrt{2}} \sin\alpha (e^{i\theta} a_- + e^{-i\theta} a_+) = 0.
\end{aligned} \tag{10}$$

Where $A_\pm(z) = a_\pm(z) e^{\pm i\varphi}, \quad A_3(z) = a_3(z), \quad \varphi = \arg k_+. \quad \theta := qz - \varphi.$ (11)

The basic solution in this case is

$$\mathbf{A}^{(n)}(k_0, \mathbf{x}) = -\frac{\omega_p}{\sqrt{2}\omega_0} e^{ik_3^{(n)}\theta/q} \left[\cos\alpha \mathbf{e}_3 + \frac{\sin\alpha}{2} \left(\frac{\omega_0^2}{\omega_0^2 - (k_3^{(n)} - q)^2} e^{-iqz} \mathbf{e}_+ + \frac{\omega_0^2}{\omega_0^2 - (k_3^{(n)} + q)^2} e^{iqz} \mathbf{e}_- \right) \right]. \tag{12}$$

Where $\mathbf{e}_\pm = \mathbf{e}_1 \pm i\mathbf{e}_2$, and $k_3^{(n)}$ are the solutions of the **dispersion equation**.

DISPERSION ANALYSIS

Dispersion relation

$$\omega_0^2\omega_p^2\sin^2\alpha(\omega_0^2-q^2-k_3^2)-\left(\omega_0^2-(k_3+q)^2\right)\left(\omega_0^2-(k_3-q)^2\right)\left(\omega_0^2-(\omega_p^2+k_3^2v^2)\cos^2\alpha\right)=0. \quad (13)$$

Asymptotic regimes

$$k_3^2+q^2\gg\omega_p^2\sin^2\alpha\,. \quad (14)$$

$$\omega_0^2(k_3)\approx\sigma_\pm^2, \qquad \sigma_\pm:=|k_3\mp q|,$$
$$\omega_0^2(k_3)\approx\sigma_p^2, \qquad \sigma_p:=\cos\alpha\sqrt{\omega_p^2+k_3^2v^2}. \quad (15)$$

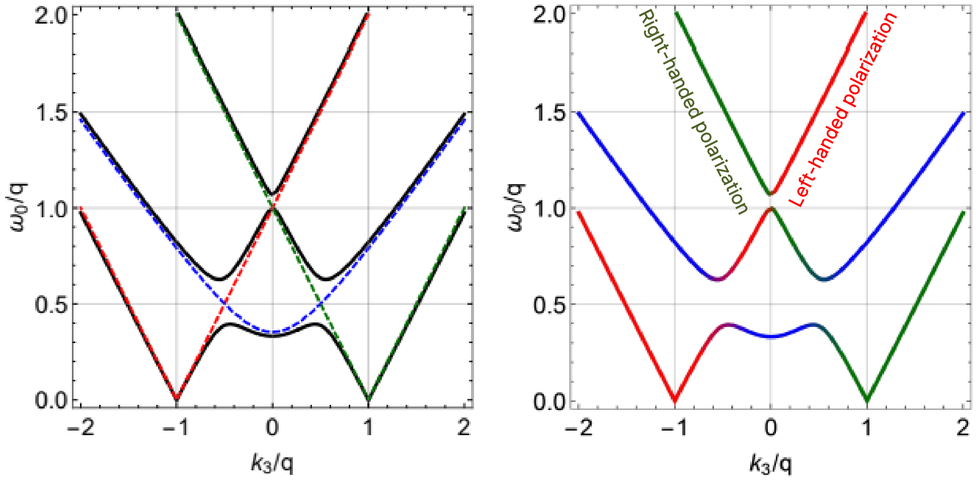


Fig. 4 $\alpha=\pi/4$, $v=1$, $\omega_p=0.5$, $\varepsilon_h=1$, and $q=1$.

$$\omega_0^2\ll\omega_p^2\cos^2\alpha, \qquad v^2k_3^2\ll\omega_p^2. \quad (16)$$

$$\omega_0^2\approx\omega_p^2+(\sin^2\alpha+v^2\cos^2\alpha)k_3^2,$$
$$\omega_0^2\approx\frac{1}{2}\Big[(1+\cos^2\alpha)(q^2+k_3^2)\pm \quad (17)$$
$$\pm\sqrt{(q^2+k_3^2)^2\sin^4\alpha+16q^2k_3^2\cos^2\alpha}\Big].$$

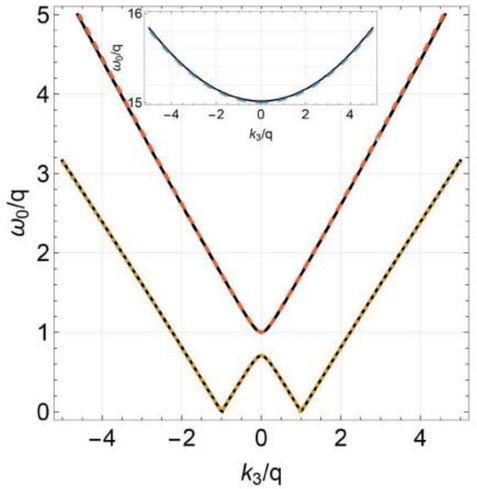


Fig. 5 $\alpha=\pi/4$, $v=1$, $\omega_p=15$, $\varepsilon_h=1$, and $q=1$.

$$|k_3|\gg|q|, \qquad \omega_p\gg|q|, \quad v=1\,. \quad (18)$$

$$\omega_0^2\approx k_3^2\cos^2\alpha, \qquad \omega_0^2\approx\omega_p^2+k_3^2,$$
$$\omega_0^2\approx k_3^2. \quad (19)$$

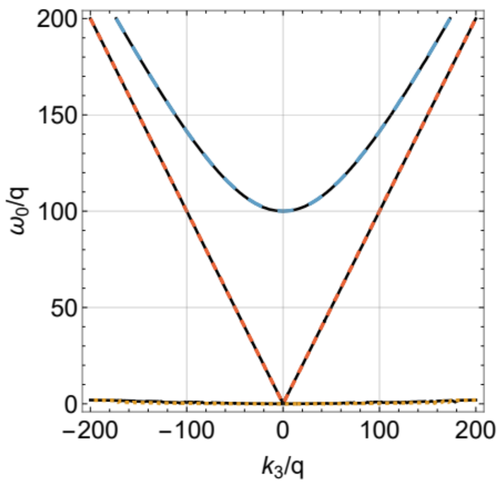
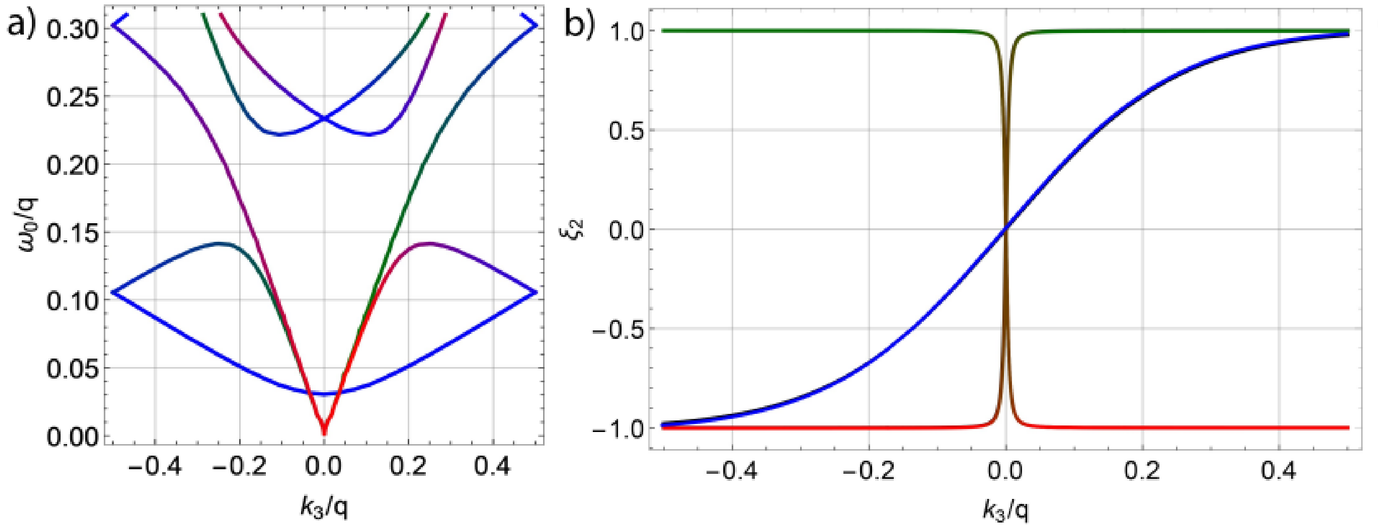


Fig. 6 $\pi/2-\alpha=0.01$, $v=1$, $\omega_p=100$, $\varepsilon_h=1$, and $q=1$.

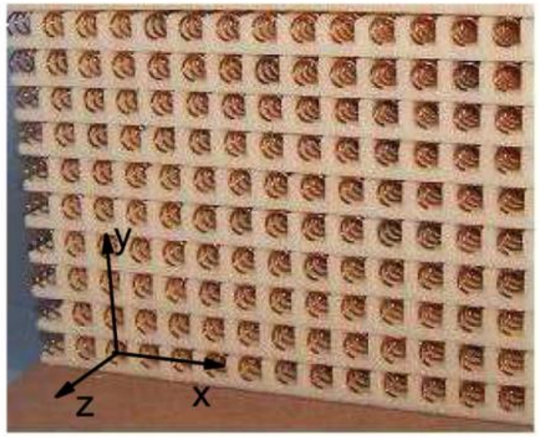
CONSISTENCY OF THE THEORY

Theory:

Fig. 7 (a) The dispersion law reduced to the first Brillouin zone in our model. (b) The degree of circular polarization for different branches of the dispersion law.



Experiment:



[C. Wu, H. Li, Z. Wei, X. Yu, and C. T. Chan, Phys. Rev. Lett. **105**, (2010).]

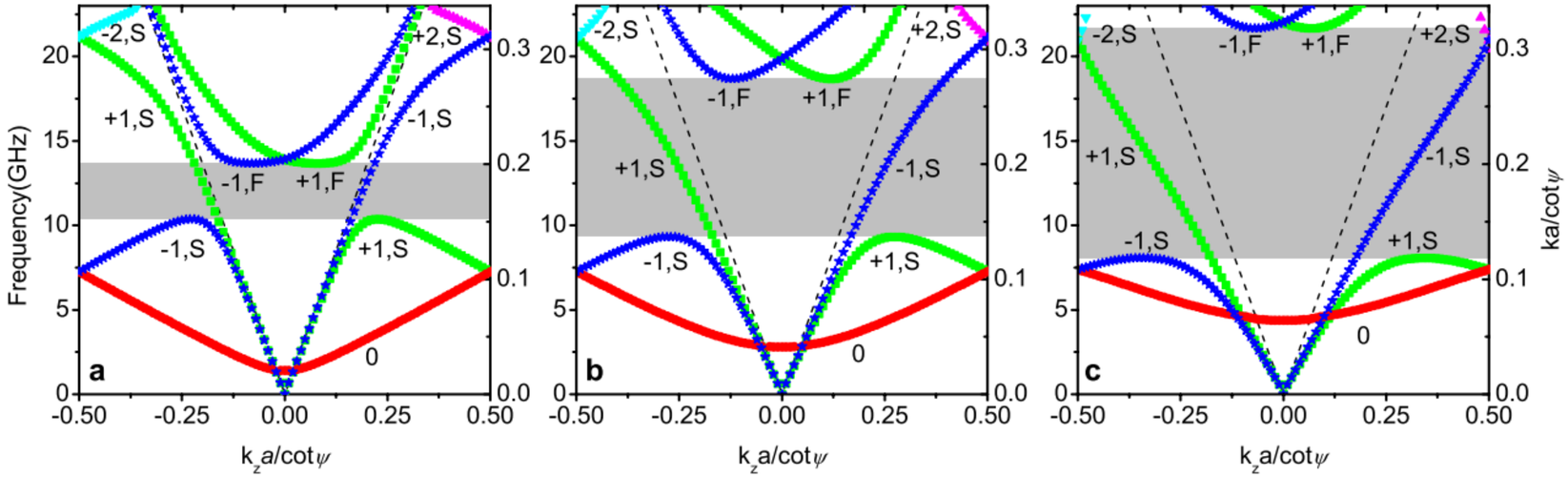


Fig. 8 Zone structure of the spiral array at normal incidence for three lattice constants (a) a=20 mm, (b) a=11 mm, (c) a=8 mm. Helical pitch p=4.4 mm, spiral radius R=3.3 mm, wire diameter δ=0.8 mm.

ENERGY FLOWS

$$\mathbf{E} = -k_0 \operatorname{Im} \mathbf{A}, \qquad \mathbf{H} = \operatorname{Re} \operatorname{rot} \mathbf{A}, \qquad \mathbf{\Pi} = [\mathbf{E}, \mathbf{H}]. \tag{20}$$

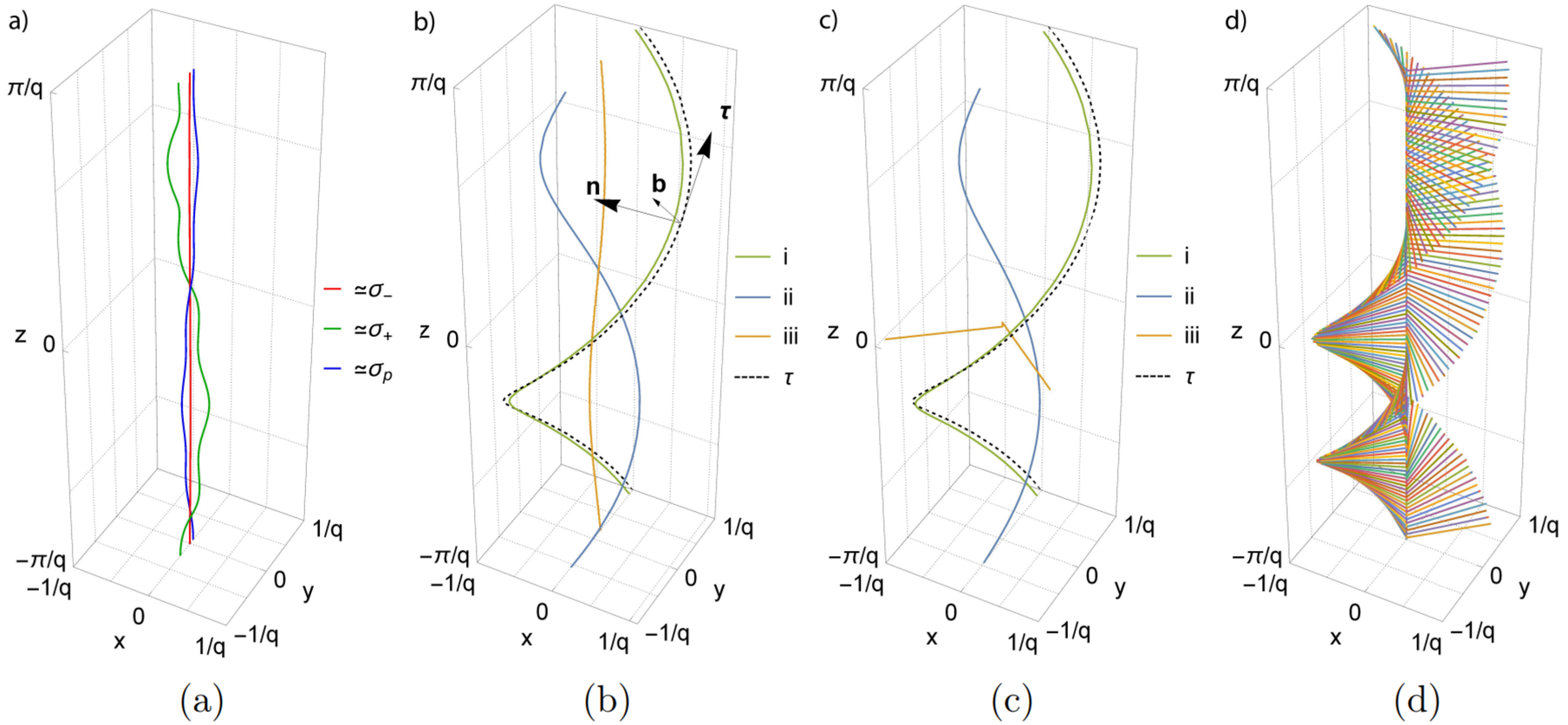
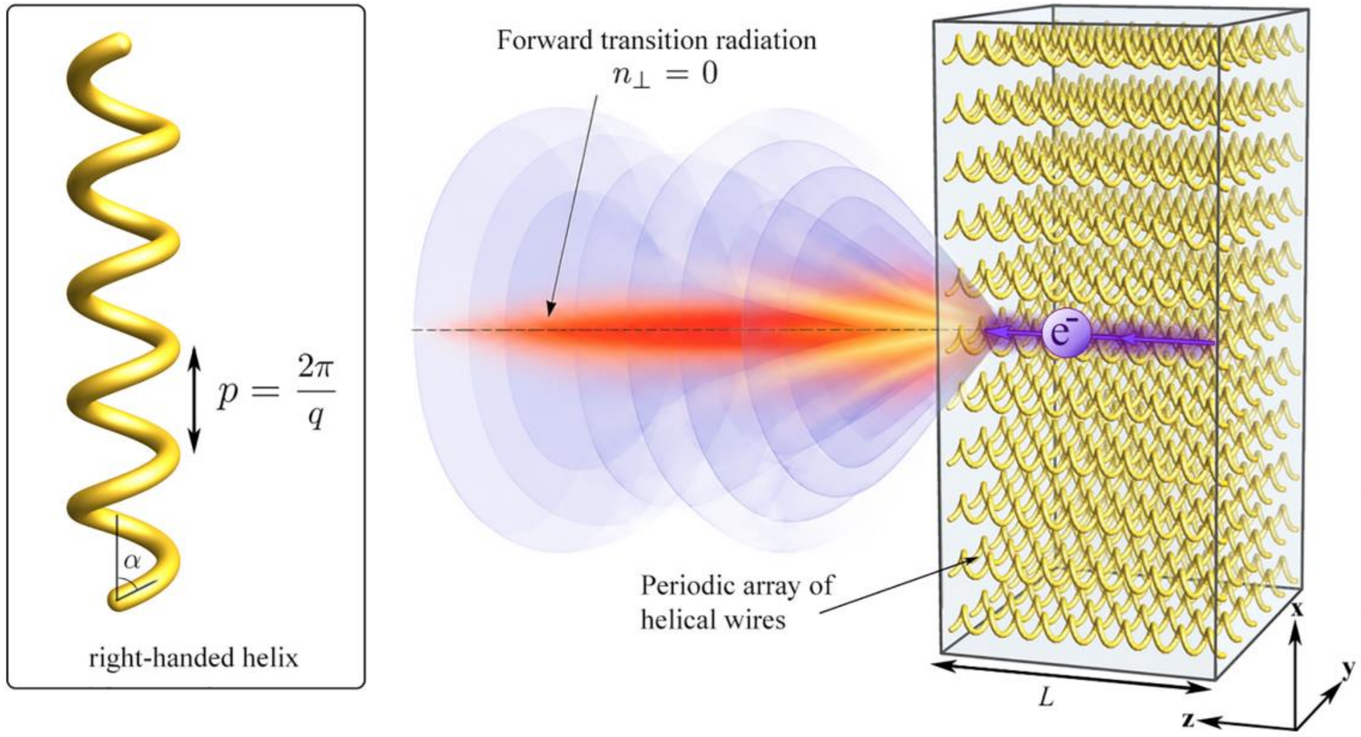


Fig. 9 Instantaneous integral curves of the Poynting vector. Graph (a): Solid lines show the integral curves of the Poynting vector for photon energies close to the asymptotics $\sigma_{\pm}, \sigma_p$. The parameter values: $\alpha = 0.25\pi, v = 1, \omega_p = 0.5, k_3 = 3, q = 1$. Graph (b): Solid lines show integral curves for parameter values: $\alpha = 0.25\pi, v = 1, \omega_p = 50, k_3 = 45, k_\perp = 0, q = 1$. The dotted line represents the integral curve of the vector $\boldsymbol{\tau}$. The vectors show the Frenet frame.. Graph (c): same as graph (b), but the parameter $k_3 = 55$. The integral curve of one of the branches of the dispersion law is degenerate. Graph (d): degenerate integral curves for different z. The parameters are the same as in graph (c). The congruence of the integral curves forms a helicoid.

RADIATION BY CHARGED PARTICLES

Using the mode functions, it is not difficult to find the average number of plane-wave photons created by a particle with charge Ze moving uniformly and rectilinearly. The trajectory of such a particle is $\mathbf{x} = \boldsymbol{\beta} t, x^0 = t.$ (21)



The average number of photons produced by the charged particle is

$$dP(s,\mathbf{k}) = Z^2 e^2 \left| \int_{-\infty}^{\infty} dt \dot{\mathbf{x}} \boldsymbol{\Phi}(s,\mathbf{k}; x(t)) \right|^2 \frac{V d\mathbf{k}}{(2\pi)^3}. \quad (22)$$

Where $\boldsymbol{\Phi}(s,\mathbf{k}; x(t))$ are joined solutions of Maxwell equations in metamaterial plate with the electromagnetic waves in vacuum.

Fig. 10 Schematic illustration of transition radiation generated by an electron moving along the symmetry axis of a helical-wire metamaterial.

RADIATION BY CHARGED PARTICLES IN A MEDIUM WITH $\omega_p = 0.5\,q$

If number of periods is large $L \gg \pi/|q|$, then the leading contribution to the radiation defined by harmonics

$$\beta_3(k_3^i + ql) + k_0(\mathbf{n}_\perp \boldsymbol{\beta}_\perp - 1) = 0 \tag{23}$$

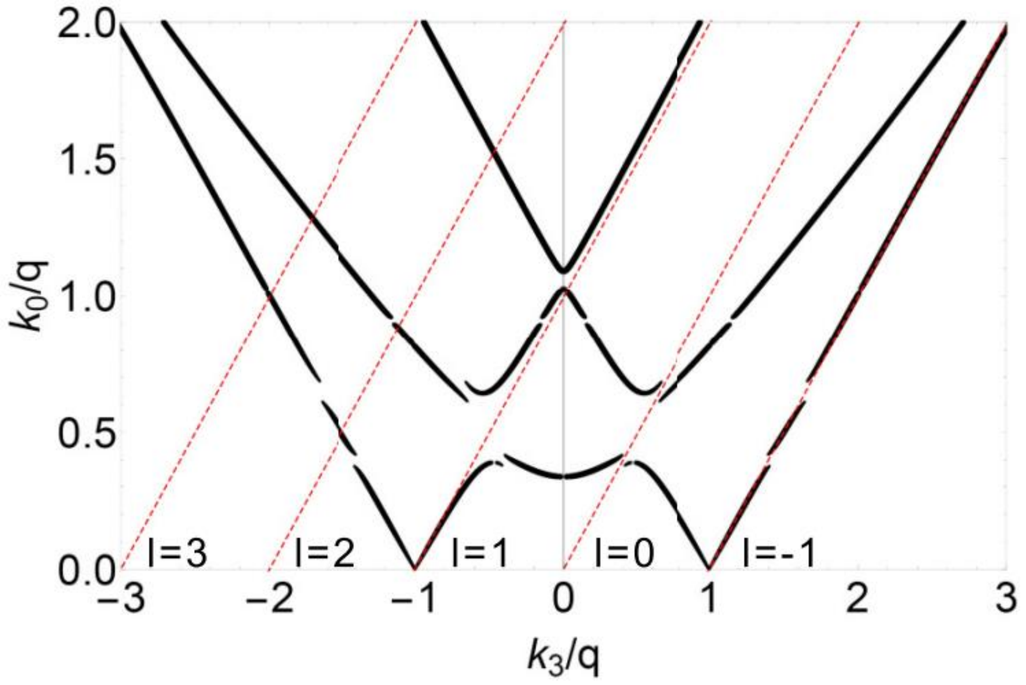


Fig. 11 The dispersion law with $\mathrm{n}_\perp = 0.2$ where the root selection procedure is applied. The electron Lorentz factor is $\gamma = 10$. The parameters of the medium are chosen as $\alpha = \frac{\pi}{4}, v = 1, \epsilon = \epsilon_h = 1, \omega_p = 0.5q$, and the specimen thickness is $\mathrm{L} = 160\pi/q$.

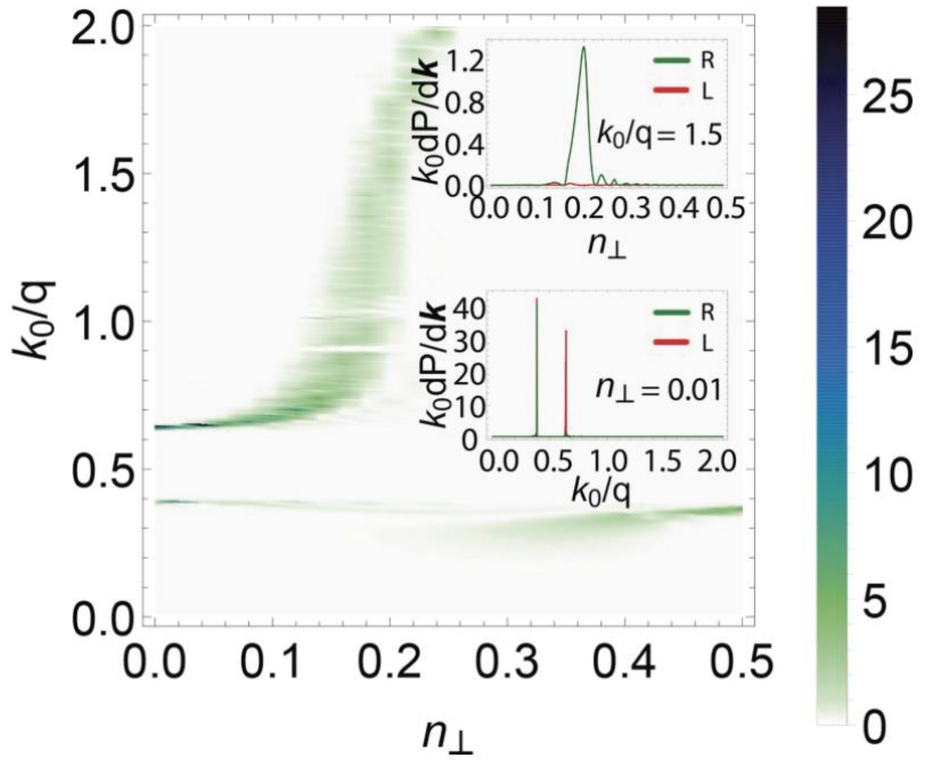


Fig. 12 The intensity of radiation of photons per volume of the cell in the momentum space from a relativistic electron with $\gamma = 10$. The parameters of the medium are chosen as $\alpha = \frac{\pi}{4}, v = 1, \epsilon = \epsilon_h = 1, \omega_p = 0.5q$, and the specimen thickness is $\mathrm{L} = 160\pi/q$.

RADIATION BY CHARGED PARTICLES IN A MEDIUM WITH $\omega_p = 1.3\,q$

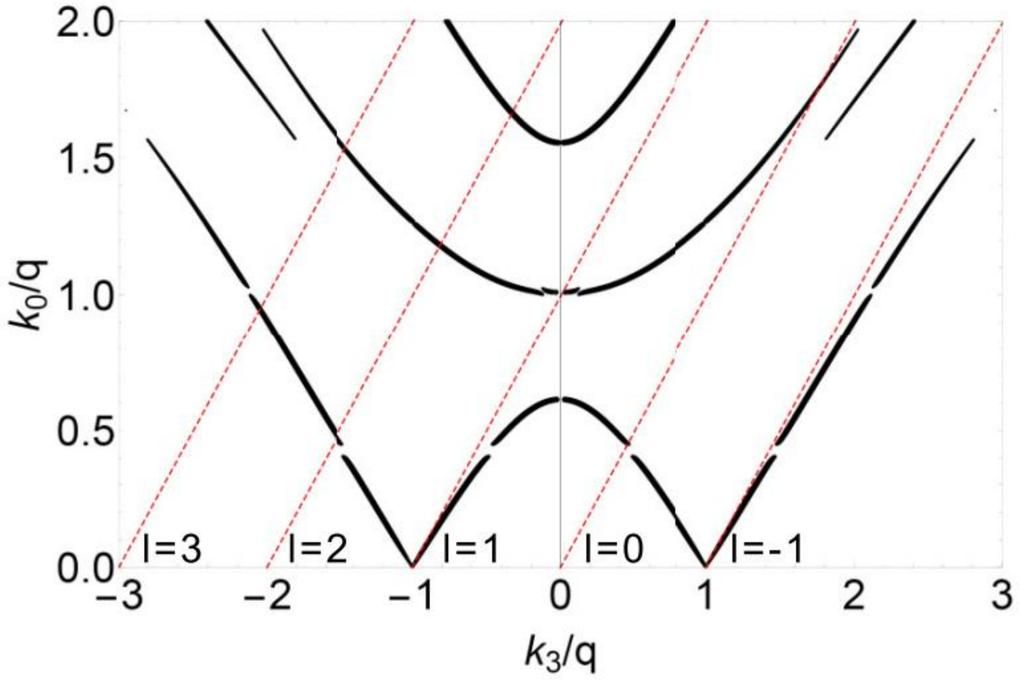


Fig. 13 The dispersion law with $\mathrm{n}_\perp = 0.2$ where the root selection procedure is applied. The electron Lorentz factor is $\gamma = 10$. The parameters of the medium are chosen as $\alpha = \frac{\pi}{4}, v = 1, \epsilon = \epsilon_h = 1, \omega_p = 1.3q$, and the specimen thickness is $\mathrm{L} = 160\pi/q$.

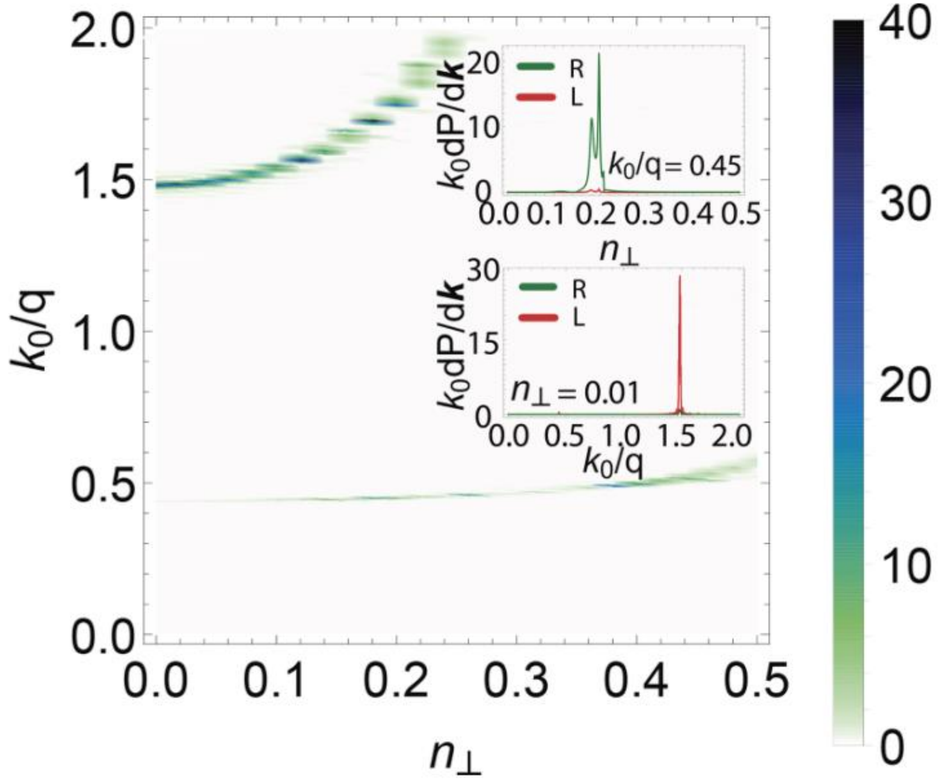


Fig. 14 The intensity of radiation of photons per volume of the cell in the momentum space from a relativistic electron with $\gamma = 10$. The parameters of the medium are chosen as $\alpha = \frac{\pi}{4}, v = 1, \epsilon = \epsilon_h = 1, \omega_p = 1.3q$, and the specimen thickness is $\mathrm{L} = 160\pi/q$.

FORWARD TRANSITION RADIATION

The radiation coming from the plasmonic branch of the dispersion law is nonzero at $n_\perp = 0$ which **is not typical** for transition and VC radiations in a medium without strong spatial dispersion.

$$dP(s,\mathbf{k}) = Z^2 e^2 \omega_p^2 \beta_3^2 \cos^2\alpha \frac{|c|^2}{\varepsilon_h} \left| \sum_{i=1}^{6} b_i \sum_{l\in\mathbb{Z}} e^{i\frac{L}{2\beta_3}x_i^l} \delta_L\left(x_i^l\right) e^{-ik_3^i\varphi/q} e^{-il\varphi} \tilde{\Psi}_i^l \right|^2 \frac{d\mathbf{k}}{8\pi k_0^3}. \qquad (24)$$

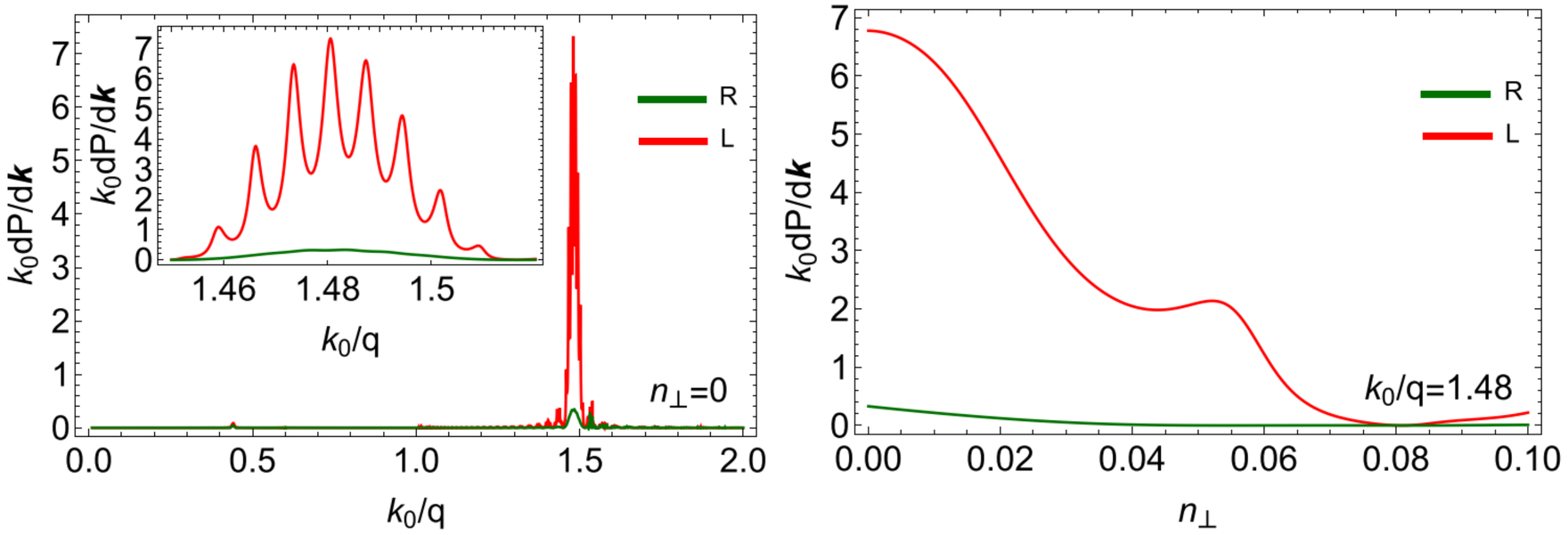


Fig. 15 The intensity of radiation of photons per volume of the cell in the momentum space from a relativistic electron with $\gamma = 10$ moving along the symmetry axis of the helical medium with strong spatial dispersion. The parameters of the medium are chosen as $\alpha = \frac{\pi}{4}, v = 1, \epsilon = \epsilon_h = 1, \omega_p = 1.3q,$

Thank you for your attention.

Speaker Petr S. Korolev

Physics Faculty, Tomsk State University

E-mail Kizorph.d@gmail.com

Acknowledgments. The study was supported by the Russian Science Foundation, grant No. 25-21-00283, https://rscf.ru/en/project/25-21-00283/